Materials Letters 176 (2016) 60–63

Contents lists available at ScienceDirect

Materials Letters

journal homepage: www.elsevier.com/locate/matlet

Preparation of activated carbon from willow leaves and evaluation in electric double-layer capacitors

Yang Liu, Yanzhong Wang*, Guoxiang Zhang, Wei Liu, Donghua Wang, Yingge Dong

School of Materials Science and Engineering, North University of China, Taiyuan 030051, PR China

ARTICLE INFO

Article history:
Received 9 October 2015
Received in revised form
31 March 2016
Accepted 9 April 2016
Available online 11 April 2016

Keywords:
Carbon materials
Porous materials
Supercapacitors
$ZnCl_2$ activation

ABSTRACT

In this paper, willow leaves were used to prepare activated carbons (ACs) by one-step pyrolysis with $ZnCl_2$ activation. The as-prepared AC-1-800 exhibits porous structure with high specific surface area of 1031 $m^2\,g^{-1}$ and a large pore volume of 0.66 $cm^3\,g^{-1}$. As a supercapacitor electrode, it shows a good capacitive performance in 6 M of KOH aqueous electrolyte, such as the specific capacitance reaches 216 $F\,g^{-1}$ at a current density of 0.1 $A\,g^{-1}$ and the retention of specific capacitance is 97% after 1000 cycles at 2 $A\,g^{-1}$.

1. Introduction

Carbon-based electrical double-layer capacitors (EDLCs) have received significant attention for their wide potential applications in electrical vehicles, digital devices and pulsing techniques due to their high durability, high power energy and fast charging-discharging mechanism [1–4]. EDLCs are generally based on the adsorption of electrolyte ions on large specific surface area conductive electrodes, in which the surface charge is separated at electrode/electrolyte interfaces. Therefore, high specific surface area and pores adapted to electrolyte ion sizes are required for EDLCs.

ACs with high specific surface area have been taken as an ideal EDLCs electrode due to their exceptional characteristics such as the moderate cost, good chemical stability and high electrical conductivity [5]. To date, the biomass-derived ACs become one of the hot topics due to their wide availability and energy/environmental concerns [6], and various biomass-derived ACs, such as from banana fibers [7], corn grain [8], starch [9], waste coffee beans [10], tea leaves [5], and dead leaves [11] have been reported. These materials have shown the great potentials to be used in supercapacitors.

Willows are widely cultivated in China as landscape and economic trees. Usually, the dead willow leaves are discarded as useless materials. Thus, it is very necessary to recycle waste willow leaves as the potential applications in energy storage. In this paper, we prepared ACs by one-step pyrolysis of willow leaves with $ZnCl_2$ activation. The as-prepared AC-1-800 exhibit porous structure with the specific surface area of 1031 $m^2\,g^{-1}$, and its capacitance reaches 216 $F\,g^{-1}$ at a current density of 0.1 $A\,g^{-1}$.

2. Experimental procedure

2.1. Materials and method

In a typical procedure, willow leaves were washed with deionized water and dried at 120 °C for 10 h. The cleaned willow leaves were cut into fine debris and mixed with $ZnCl_2$ (the weight ratios of $ZnCl_2$ to willow leaves are 0.5, 1 and 3), and pyrolyzed under nitrogen atmosphere at 700–900 °C for 2 h with a heating rate of 5 °C min^{-1}. The resulting dark solid was washed with 2 M HCl solution, and then washed with deionized water and ethanol, respectively. The residue was collected and dried at 110 °C for 10 h in a vacuum oven. The as-prepared willow leaves-derived ACs are denoted as AC-*x*-T, where *x* indicates the weight ratio of $ZnCl_2$ to willow leaves, and T indicates the carbonization temperature.

2.2. Characterizations

X-ray diffraction (XRD) analysis of activated carbons was performed at room temperature with Cu K_a radiation. The data were collected in the 2θ-range from 20 to 80° with a step size of 0.02°. The morphologies of samples were characterized by scanning electron microscope (SEM, Hitachi S-4700). The nitrogen adsorption-desorption isotherm measurements were performed on a

* Corresponding author.
E-mail address: wyzletter@nuc.edu.cn (Y. Wang).

http://dx.doi.org/10.1016/j.matlet.2016.04.065
0167-577X/

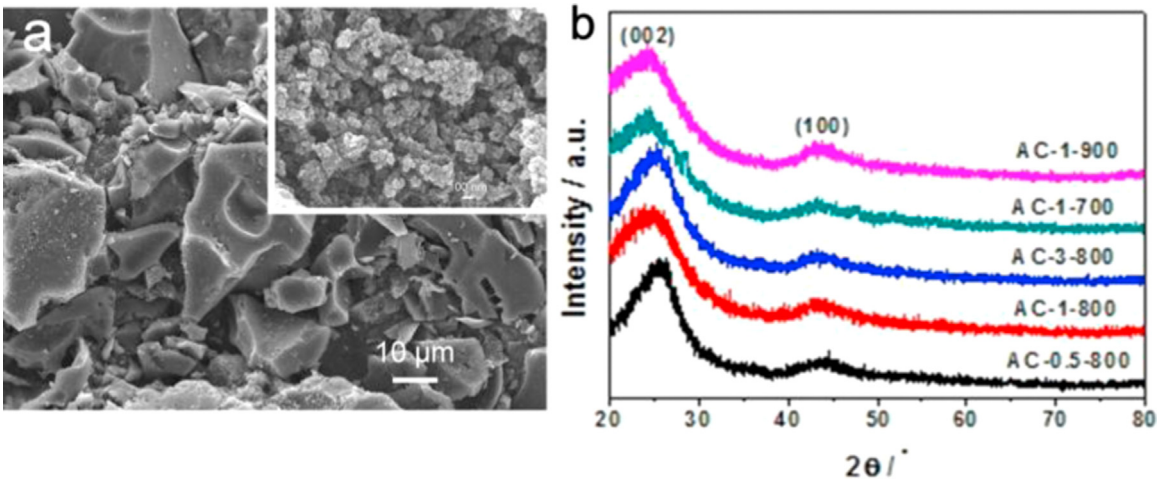

Fig. 1. (a) SEM images of AC-1-800, (b) XRD patterns of all samples.

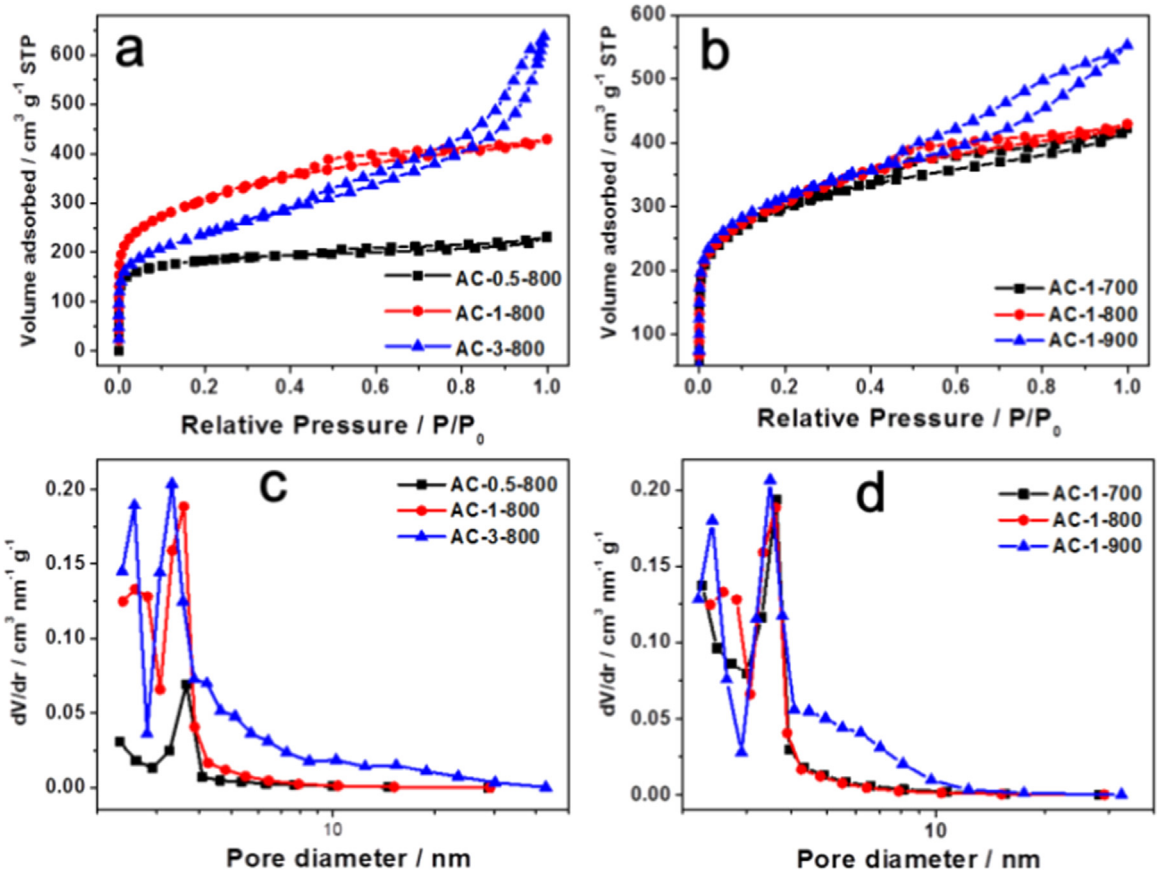

Fig. 2. (a) and (b) Nitrogen sorption isotherms of samples, (c) and (d) BJH pore size distributions.

Table 1
The pore structure and capacitance of samples.

Samples	S_{BET} ($m^2\ g^{-1}$)	V_{pore} ($cm^3\ g^{-1}$)	V_{mes} ($cm^3\ g^{-1}$)	D_{aver} (nm)
AC-0.5-800	587	0.359	0.111	2.521
AC-1-800	1031	0.664	0.375	4.309
AC-3-800	809	0.986	0.844	6.323
AC-1-700	1002	0.653	0.346	3.831
AC-1-900	1065	0.856	0.546	4.640

Micromeritics ASAP 2020 M volumetric adsorption analyzer at 77 K. The Brunauer-Emmett- Teller (BET) method was utilized to calculate the specific surface area.

2.3. Electrochemical measurement

The electrochemical measurements were conducted in a three-electrode system in 6 M KOH aqueous electrolyte. A platinum foil

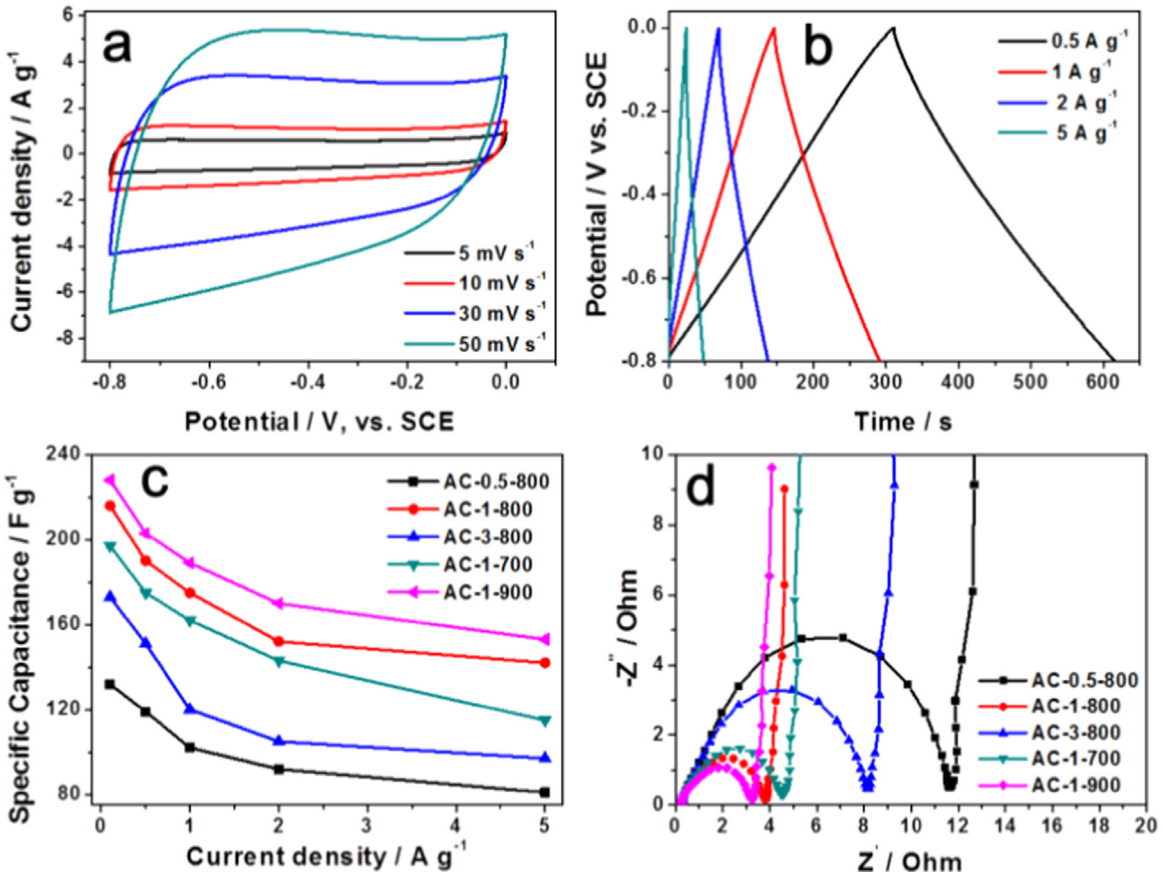

Fig. 3. (a) CV curves of AC-1-800 at different scan rates, (b) GCD curves of AC-1-800 at different current densities, (c) the specific capacitance of samples at different current densities, (d) Nyquist plots of samples.

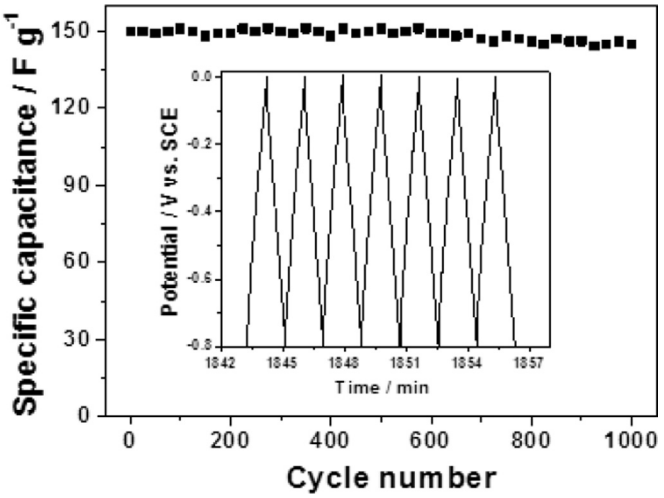

Fig. 4. The cycling performance of AC-1-800 at the current density of 2 A g^{-1}, and the inset shows the charge/discharge curves of the 7 cycles of the electrode.

and saturated calomel electrode (SCE) were used as the counter electrode and reference electrode, respectively. The working electrode was prepared by mixing the activated carbons, acetylene black and polytetrafluoroethylene (PTFE) at a weight ratio of 85:10:5. The above materials (6 mg) were coated onto a 1 cm × 1 cm nickel foam, and dried at 110 °C for 12 h. The capacitive performances of samples were investigated by cyclic voltammeter (CV), galvanostatic charge-discharge (GCD), and electrochemical impedance spectroscopy (EIS) techniques using an electrochemical workstation (Bio-logic SP 200). The specific capacitance of samples was calculated using the following equation Eq. (1):

$$C = I\Delta t/(m\Delta V) \quad (1)$$

where C is the specific capacitance (F g^{-1}), I is the discharge current (A), Δt is the discharge time (s), m is the mass of the active material in the electrode (g), and ΔV is the potential change in discharge (V).

3. Results and discussion

The porous activated carbons derived from willow leaves were prepared by one-step pyrolysis under nitrogen atmosphere with $ZnCl_2$ activation. Among the chemical activators, it is widely recognized that $ZnCl_2$, a Lewis acid, acts as both a template and activating agent that promotes the decomposition of carbonaceous material during the pyrolysis process, restricts the formation of tar, and increases the carbon yield and specific surface area [12]. All as-prepared ACs show the similar microstructure, and the representative SEM image of AC-1-800 is shown in Fig. 1a. The porous graphite flakes were observed, and the magnified view in the inset shows that they were composed of nanometer-sized spherical particles. The XRD patterns of ACs at different carbonization temperatures are shown in Fig. 1b. It is clearly seen that all as-prepared ACs possess a well-developed graphitic stacking peak at 22.3°, and a weak peak at 43.8°due to the formation of a high degree of interlayer condensation, which should greatly improve the electrical conductivity [13]. No peaks related to ZnO or Zn

$(OH)_2$ were detected.

The pore structures of samples were investigated using N_2 adsorption-desorption isotherm measurement (Fig. 2). The isotherms of ACs exhibit type IV according to the IUPAC classification, and the hysteresis loops were observed above 0.45, which are characteristic of mesoporous materials [14]. Table 1 shows that the pore volume and average pore sizes increase with increasing $ZnCl_2$ contents, but the specific surface area of AC-1-800 is higher than that of AC-0.5-800 and AC-3-800. The specific surface area, pore volume and average pore size increase with increasing heating temperature, such as AC-1-900 shows the maximum specific surface area ($1065\ m^2\ g^{-1}$). At high $ZnCl_2$ ratio (>1), some $ZnCl_2$ compounds remain in the external part of the carbon particles, widening the pore by a localized decomposition of the organic matter rather than the creation of additional micropores. This process results in the enhancement of the meso- and macro-pore formation [15]. Khalili et al. [16] also observed that at $ZnCl_2$ ratio in the range from 1 to 2, the creation and widening of micropores take place simultaneously. When the $ZnCl_2$ ratio is higher than 2, the pore widening becomes the dominant mechanism and the mesopores are formed.

The capacitive performances of ACs are shown in Fig.3. The CV curves of AC-1-800 exhibit a well-defined rectangle at the scan rate range from 5 to 50 mV s^{-1} (Fig. 3a) indicating a typical EDLCs behavior [17]. Fig. 3b exhibits the GCD curves of AC-1-800 at the different current densities. The specific capacitance was calculated by Eq. (1), and the values are shown in Fig. 3c. The specific capacitances of ACs are in the range from 138 to 228 F g^{-1} at the current density of 0.1 A g^{-1}. The specific capacitance of AC-1-900 is still remained at 153 F g^{-1} even at a high current density of 5 A g^{-1}. Fig. 3d shows the Nyquist plots of samples at the frequency range from 10^{-2} to 10^5 Hz. In the low frequency region, the electrodes exhibit a vertical line parallel to the imaginary axis, indicating a good capacitive behavior. In the high frequency region, the real axis intercept is the equivalent series resistance (R_s), and the width of the semicircle impedance loop represents the charge-transfer resistance [18]. Although R_s of all samples is about 0.2 Ω, the ion-transport resistances of ACs decrease with increasing the carbonization temperature, suggesting that the high carbonization temperature benefits the effective ion migration into the electrode.

The cycling stability determine the practical application of supercapacitors. Fig. 4 shows the cycling performance of AC-1-800 after 1000 successive charging-discharging cycles at a current density of 2 A g^{-1}. The specific capacitance decreased slowly at initial stage and then tends to be stable at 97% of the initial capacitance, indicating the excellent cycling stability of AC-1-800 as supercapacitor electrode materials.

4. Conclusions

Porous ACs were prepared by one-step pyrolysis of willow leaves with $ZnCl_2$ chemical activation at 700–900 °C for 2 h under N_2 atmosphere. The specific surface area of ACs increases with increasing the carbonization temperature. When the weight ratio of $ZnCl_2$ to willow leaves is 1 and the carbonization temperature is 800 °C, the AC-1-800 exhibits the high specific surface area of $1031\ m^2\ g^{-1}$, and its capacitance reaches 216 F g^{-1} at current density of 0.1 A g^{-1}. The long term performance maintains at about 97% of the initial capacitance after 1000 cycles, indicating its excellent stability as supercapacitor electrode.

Acknowledgement

This work was financially supported by the National Natural Science Foundation of China (No. 51102216), the Natural Science Foundation for Young Scientists of Shanxi Province (No. 2012021021-1).

References

[1] A. Ghosh, Y.H. Lee, Chem. Sus. Chem. 5 (2012) 480–499.
[2] C. Merlet, B. Rotenberg, P.A. Madden, P.L. Taberna, P. Simon, Y. Gogotsi, et al., Nat. Mater. 11 (2012) 306–310.
[3] Y. Zhu, S. Murali, M.D. Stoller, K.J. Ganesh, W. Cai, P.J. Ferreira, et al., Science 332 (2011) 1537–1541.
[4] C. Guan, X. Xia, N. Meng, Z. Zeng, X. Cao, C. Soci, et al., Energy Env. Sci. 5 (2012) 9085–9090.
[5] C. Peng, X.B. Yan, R.T. Wang, J.W. Lang, Y.J. Ou, Q.J. Xue, Electro. Acta 87 (2013) 401–408.
[6] R. Wang, P. Wang, X. Yan, J. Lang, C. Peng, Q. Xue, ACS Appl. Mater. Inter 4 (2012) 5800–5806.
[7] V. Subramanian, C. Luo, A.M. Stephan, K.S. Nahm, S. Thomas, B.J. Wei, Phys. Chem. C 111 (2007) 7527–7531.
[8] M.S. Balathanigaimani, W.G. Shim, M.J. Lee, C. Kim, J.W. Lee, H. Moon, Electrochem. Commun. 10 (2008) 868–871.
[9] Q.Y. Li, H.Q. Wang, Q.F. Dai, J.H. Yang, Y.L. Zhong, Solid State Ion. 179 (2008) 269–273.
[10] T.E. Rufford, D. Hulicova-Jurcakova, Z. Zhu, G.Q. Lu, Electrochem. Commun. 10 (2008) 1594–1597.
[11] M. Biswal, A. Banerjee, M. Deo, S. Ogale, Energy Env. Sci. 6 (2013) 1249–1259.
[12] F. Cesano, M.M. Rahman, S. Bertarione, J.G. Vitillo, D. Scarano, A. Zecchina, Carbon 50 (2012) 2047–2051.
[13] J.P. Paraknowitsch, J. Zhang, D. Su, A. Thomas, Adv. Mater. 22 (2010) 87–92.
[14] T.E. Rufford, D. Hulicova-Jurcakova, K. Khosla, Z. Zhu, G.Q. Lu, J. Power Sources 195 (2010) 912–918.
[15] T.E. Rufford, D. Hulicova-Jurcakova, E. Fiset, Z. Zhu, G.Q. Lu, Electrochem. Commun. 11 (2009) 974–977.
[16] N.R. Khalili, M. Campbell, G. Sandi, J. Golaś, Carbon 38 (2000) 1905–1915.
[17] F. Zhou, Q. Liu, D. Kang, J. Gu, W. Zhang, D. Zhang, J. Mater. Chem. A 2 (2014) 3505–3512.
[18] L. Sun, C. Tian, M. Li, X. Meng, L. Wang, R. Wang, et al., J. Mater. Chem. A 1 (2013) 6462–6470.